High-energy high-luminosity electron-ion collider eRHIC

Vladimir N. Litvinenko, Ilan Ben-Zvi, Lee Hammons, Yue Hao, and Stephen Webb
Brookhaven National Laboratory, Upton, NY 11973 and
Department of Physics and Astronomy, Stony Brook University, Stony Brook 11784
Joanne Beebe-Wang, Sergey Belomestnykh, Michael M. Blaskiewicz, Rama Calaga, Xiangyun Chang, Alexei Fedotov, David Gassner, Harald Hahn, Ping He, William Jackson, Animesh Jain, Elliott C.Johnson, Dmitry Kayran, Jorg Kewisch, Yun Luo, George Mahler, Gary McIntyre, Wuzheng Meng, Michiko Minty, Brett Parker, Alexander Pikin, Vadim Ptitsyn, Triveni Rao, Thomas Roser, John Skaritka, Brian Sheehy, Steven Tepikian, Yatming Than, Dejan Trbojevic, Nicholaos Tsoupas, Joseph Tuozzolo, Gang Wang, Qiong Wu, Wencan Xu, and Anatoly Zelenski
Brookhaven National Laboratory, Upton, NY 11973
Eduard Pozdeyev
FRIB, Michigan State University, East Lansing, MI 48824
Evgeni Tsentalovich
MIT-Bates, Middleton, MA 01949

1. Introduction

In this paper, we describe a future electron-ion collider (EIC), based on the existing Relativistic Heavy Ion Collider (RHIC) hadron facility, with two intersecting superconducting rings, each 3.8 km in circumference [1]. The replacement cost of the RHIC facility is about two billion US dollars, and the eRHIC will fully take advantage and utilize this investment. We plan adding a polarized 5-30 GeV electron beam to collide with variety of species in the existing RHIC accelerator complex, from polarized protons with a top energy of 325 GeV, to heavy fully-striped ions with energies up to 130 GeV/u.

Brookhaven's innovative design, (Fig. 1), is based on one of the RHIC's hadron rings and a multi-pass energy-recovery linac (ERL). Using the ERL as the electron accelerator assures high luminosity in the $10^{33} - 10^{34}$ cm^{-2} sec^{-1} range, and for the natural staging of eRHIC, with the ERL located inside the RHIC tunnel. The eRHIC will provide electron-hadron collisions in up to three interaction regions. We detail the eRHIC's performance in Section 2.

Since first paper on eRHIC paper in 2000, its design underwent several iterations. Initially, the main eRHIC option (the so-called ring-ring, RR, design) was based on an electron ring, with the linac-ring (LR) option as a backup. In 2004, we published the detailed "eRHIC 0th Order Design Report" [2] including a cost-estimate for the RR design. . After detailed studies, we found that an LR eRHIC has about a 10-fold higher luminosity than the RR. Since 2007, the LR, with its natural staging strategy and full transparency for polarized electrons, became the main choice for eRHIC. In 2009, we completed technical studies of the design and dynamics for MeRHIC with 3-pass 4 GeV ERL. We learned much from this evaluation, completed a bottom-up cost estimate for this $350M machine, but then shelved the design.

In the same year, we turned again to considering the cost-effective, all-in-tunnel six-pass ERL for our design of the high-luminosity eRHIC (Fig.1). In it, electrons from the polarized pre-injector will be accelerated to their top energy by passing six times through two SRF linacs. After colliding with the hadron beam in up to three detectors, the e-beam will be decelerated by the same linacs and dumped. The six-pass magnetic system with small-gap magnets [3] will be installed from the start. We will stage the electron energy from 5 GeV to 30 GeV stepwise by increasing the lengths of the SRF linacs. We discuss details of eRHIC's layout in Section 3.

We considered several IR designs for eRHIC. The latest one, with a 10 mrad crossing angle and $\beta^* = 5$ cm, takes advantage of newly commissioned Nb_3Sn quadrupoles [4]. Section 4 details the eRHIC lattice and the IR layout.

The current eRHIC design focuses on electron-hadron collisions. If justified by the EIC physics, we will add a 30 GeV polarized positron ring with full energy injection from eRHIC ERL. This addition to the eRHIC facility provide for positron-hadron collisions, but at a significantly lower luminosity than those attainable in the electron-hadron mode.

As a novel high-luminosity EIC, eRHIC faces many technical challenges, such as generating 50 mA of polarized electron current. eRHIC also will employ coherent electron cooling (CeC) [5] for the hadron beams. Staff at BNL, JLab, and MIT is pursuing vigorously an R&D program for resolving addressing these obstacles. . In collaboration with Jlab, BNL plans experimentally to demonstrate CeC at the RHIC. We discuss the structure

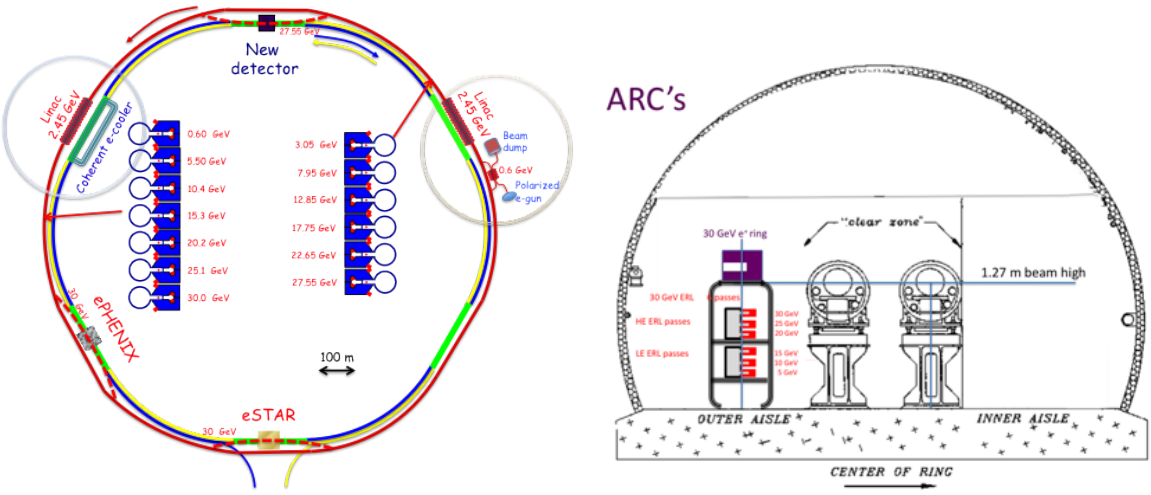

(a) (b)

Figure 1: (a) Layout of the ERL based, all-in-RHIC-tunnel, 30 GeV x 325 GeV high-energy high-luminosity eRHIC. (b) Location of six eRHIC's recirculation arcs in RHIC tunnel.

and the status of the eRHIC R&D in Section 5.

2. Main eRHIC parameters

eRHIC is designed to collide electron beams with energies from 5 to 30 GeV[1] with hadrons, viz., either with heavy ions having energies from 50 GeV to 130 GeV per nucleon or with polarized protons with energies between 100 and 325 GeV. It means that eRHIC will cover the C.M. energy range from 44.7 GeV to 197.5 GeV for polarized e-p, and from 31.6 GeV to 125 GeV for electron heavy-ion collisions.

Present top energy of RHIC is 250 GeV for polarized protons and 100 GeV/u for heavy ions. We are considering a possibility of increasing these energies for up to 30%. This increase is not a certainty and is a subject of dedicated studies at RHIC.

Several physics and practical considerations influenced our choice of beam parameters for eRHIC. Some of these limitations, such as the intensity of the hadron beam , the space charge and beam-beam tune shift limits for hadrons, come from experimental observations at RHIC or other hadron colliders. Some of them, for example $\beta^* = 5$ cm for hadrons, are at the limits of current accelerator technology, while others are derived either from practical or cost considerations.

For example, from considering the operational costs, we limit the electron beam's power loss for synchrotron radiation to about 7 MW, corresponding to a 50 mA beam current at 20 GeV. Above 20 GeV, the electron beam's current will decrease in inverse proportion to the fourth power of energy, and will be restricted to about 10-mA at energy of 30 GeV. It means that the luminosity of eRHIC operating with 30 GeV electrons will be a $1/5^{th}$ of that with 20 GeV.

Since the ERL provides fresh electron bunch at every collision, the electron beam can be strongly abused, i.e., it can heavily distorted during collision. The only known effect that might cause a serious problem is the so-called kink instability. The ways of suppressing it within range of parameters accessible by eRHIC is well-understood [6] and it no longer presents a problem.

We list below some of our assumed limits and parameters:

1. Bunch intensity limits:

   (a) For protons: 2×10^{11};

[1]There is no accelerator problem with using lower energy electron beams. According to statements by EIC physicists, using electron energies below 5 GeV would not contribute significantly to the physics goals.

Table I: Projected eRHIC luminosity for various hadron beams at top energy.

	e	p	$^{2}He^{3}$	$^{79}He^{197}$	$^{92}He^{238}$
Energy, GeV	5-20	325	215	130	130
CM energy, GeV		80-161	131	102	102
Number of bunches (ions) / distance between bunches (electrons)	74 nsec	166	166	166	166
Bunch intensity ($\times 10^{11}$ nucleons)	0.24	2	3	3	3.15
Bunch charge, nC	3.8	32	30	19	20
Beam current, mA	50	420	390	250	260
Normalized emittance of hadrons 95%, mm mrad		1.2	1.2	1.2	1.2
Normalized emittance of electrons rms, mm mrad		5.8-23	7-35	12-57	12-57
Polarization, %	80	70	70	none	none
RMS bunch length, cm	0.2	4.9	8.3	8.3	8.3
β^*, cm	5	5	5	5	5
Luminosity per nucleon, 10^{34} $cm^{-2}s^{-1}$		1.46	1.39	0.86	0.92

Table II: Projected eRHIC luminosity (in 10^{33} $cm^{-2}sec^{-1}$) for polarized electron and proton collisions.

	Protons			
Electrons	100 GeV	130 GeV	250 GeV	325 GeV
5 GeV	0.62	1.4	9.7	15
10 GeV	0.62	1.4	9.7	15
20 GeV	0.62	1.4	9.7	15
30 GeV	0.62	0.35	2.4	3.8

(b) For Au ions: 1.2×10^9

2. Electron current limits:

   (a) Polarized current: 50 mA;

   (b) Unpolarized current 250 mA

3. 3. Minimum $\beta^* = 5$ cm for all species

4. Space charge tune shift limit for hadrons: ≤ 0.035

5. Proton (ion) beam-beam parameter: ≤ 0.015

6. Bunch length (with coherent electron cooling):

   (a) Proton: 8.3 cm at energies below 250 GeV, 4.9 cm at 325 GeV ;

   (b) Au ion: 8.3 cm in all energy range

7. Synchrotron radiation intensity limit is defined as that of 50 mA beam at 20 GeV

8. Collision rep-rate $\leq$ 50 MHz.

The limitations on luminosity resulting from various considerations are involved. The main trend is that eRHIC's luminosity does not depend on the electron beam's energy (below 20 GeV), and reaches its maximum at the hadron beam's highest energy. We mentioned the exception for energies of electrons above 20 GeV. Table 1 gives the top eRHIC performance for various species is shown in Table 1.

Table 2 lists the luminosity of a polarized electron-proton collision for a set of electron and proton energies.

Table 3 contains the same information for a polarized electron beam colliding with Au ions, while Tables 4 and 5 provide data for the case of unpolarized electrons.

Table III: Projected eRHIC luminosity (in 10^{33} cm^{-2}sec^{-1}) for polarized electrons and Au ions.

	Ions			
Electrons	50 GeV	75 GeV	100 GeV	130 GeV
5 GeV	0.49	1.7	3.9	8.6
10 GeV	0.49	1.7	3.9	8.6
20 GeV	0.49	1.7	3.9	8.6
30 GeV	0.13	0.43	0.8	2.1

Table IV: Projected eRHIC luminosity (in 10^{33} cm^{-2}sec^{-1}) for unpolarized electron and polarized proton collisions.

	Protons			
Electrons	100 GeV	130 GeV	250 GeV	325 GeV
5 GeV	3.1	5	9.7	15
10 GeV	3.1	5	9.7	15
20 GeV	0.62	1.4	9.7	15
30 GeV	0.15	0.35	2.4	3.8

An additional major parameter describing eRHIC's overall performance is its expected average luminosity. Since the plans for eRHIC are to use coherent electron cooling to control the parameters of hadron beam, its lifetime will be affected only by scattering on residual gas, and by burn-off in collisions with electrons. Hence, the hadron beam's luminosity lifetime could be as long as few days, and, in the most likely scenario, the average delivered luminosity will be determine by the reliability of RHIC systems. Hence, we anticipate that the average luminosity will be $\sim 70\%$ of that listed in the tables.

3. eRHIC layout and dynamics

Injector. As shown in Fig.1, an electron gun will provide fresh electron beams. We will employ a 50-mA polarized electron gun, based either on single large-sized GaAs cathode [7] (Fig. 2 (a)), or on a Gatling gun [8,9] an approach combining beams from a large array of GaAs cathodes (Fig.2 (b)).

Illuminated by circular polarized IR laser light a strained or super-lattice GaAs cathode will produce longitudinally of highly polarized electrons. The polarization of electrons can be as high as 85-90%. The direction of electron's spin can be flipped on the bunch-to-bunch basis by changing the helicity of the laser photons.

We will utilize a dedicated un-polarized SRF electron gun, similar to that designed for BNL's R&D ERL [10] to generate a significantly higher beam current (up to 250 mA CW).

Thereafter, the electrons will be accelerated in a pre-injector linac and then will go six times around RHIC tunnel, gaining energy from two super-conducting RF (SRF) linacs located in two of the RHIC straight sections (see Fig. 1a, where linacs are located at 2 and 10 o'clock straight sections). They can accommodate SRF 703 MHz linacs up to maximum length of 201 m, which suffices for a 2.45-GeV linac operating with a real-estate gradient of 12.45 MeV per meter, corresponding to 20.4-MeV gain per 5-cell 703 MHz cavity.

The Main ERL. While the magnets for the six passes around the eRHIC will be installed from the start, the top energy of electron beam will be raised in stages by increasing the length (and the energy gains) of each linac in the ERL chain. At the final stage, the two main linacs each will have energy gain of 2.45 GeV, while the injection SRF linac will provide 0.6 GeV of energy. At all intermediate stages, the energy gains of all linacs will be proportionally lower, i.e., for the10-GeV stage, the e-beam will be injected at 0.2-GeV into the main ERL, and each main linac will provide an 0.817 GeV energy gain..

Table V: Projected eRHIC luminosity (in 10^{33} cm^{-2}sec^{-1}) for unpolarized electron and Au ion collisions.

	Ions			
Electrons	50 GeV	75 GeV	100 GeV	130 GeV
5 GeV	2.5	8.3	11.4	18
10 GeV	2.5	8.3	11.4	18
20 GeV	0.49	1.7	3.9	8.6
30 GeV	0.1	0.34	0.77	1.7

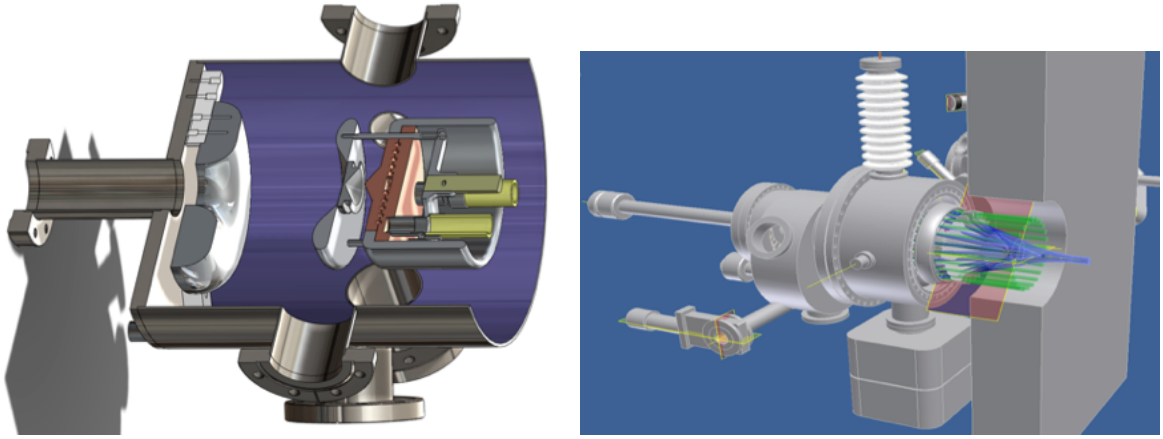

(a) (b)

Figure 2: Two candidates for eRHIC polarized electron gun: (a) with a large-size GaAs cahthode gun; (b) Gutling gun combing beams from the array of 24 GaAs cathodes.

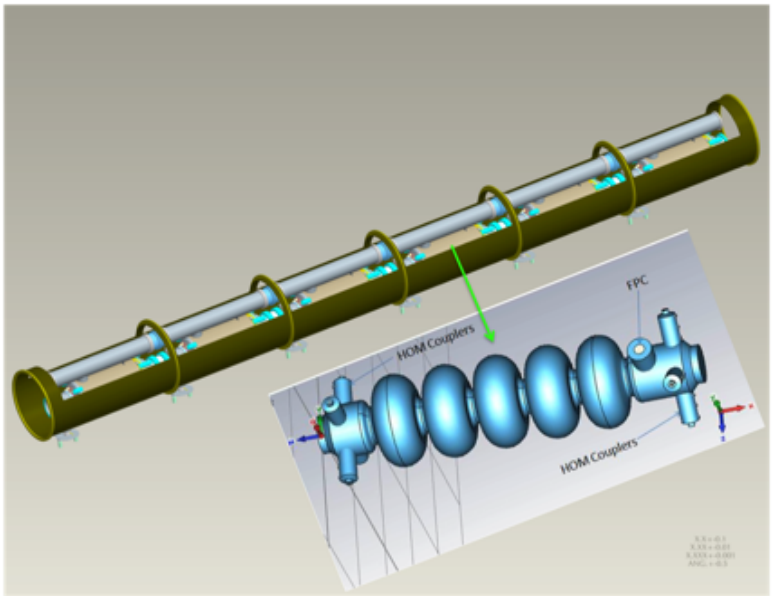

Figure 3: An eRHIC SRF cyro-module with 5-cell SRF cavities (insert)

We plan to build the eRHIC's linacs from modules comprising 5-cell 703 MHz SRF cavities. Fig.3 is a 3D rendering of such modules, and of the 5-cell cavity model with HOM dumpers.

At their peak energy, the electrons collide with hadrons and then their energy is recovered by the same linacs. The latter process is assured by additional 180 degrees delay of the electrons at the top energy, such a delay switches the acceleration to deceleration.

Beams at all energies pass through the same linacs while propagating in their individual beam-lines around the arcs. This feature is achieved via dedicated combiners and splitters. Fig.4 depicts the arrangement in the 10 o'clock straight section; a similar system is located in the 2 o'clock section.

Except at their top energy, the accelerating and decelerating beams share the arcs, though separated in time. For example, electron beams at 15.3 GeV traverse the same arc between IP2 and IP10, wherein the energy of accelerating beam increases to 17.75 GeV. It enters a 17.75 GeV arc together with the beam that just was decelerated from 20.2 GeV. In contrast, after passing through the linac, the decelerating 15.3 GeV beam passes into the 12.85 GeV arc sharing it with the beam that was just accelerated in the same linac from 10.4 GeV. This important ratio between accelerating and decelerating beams is maintained with two linacs having equal energy

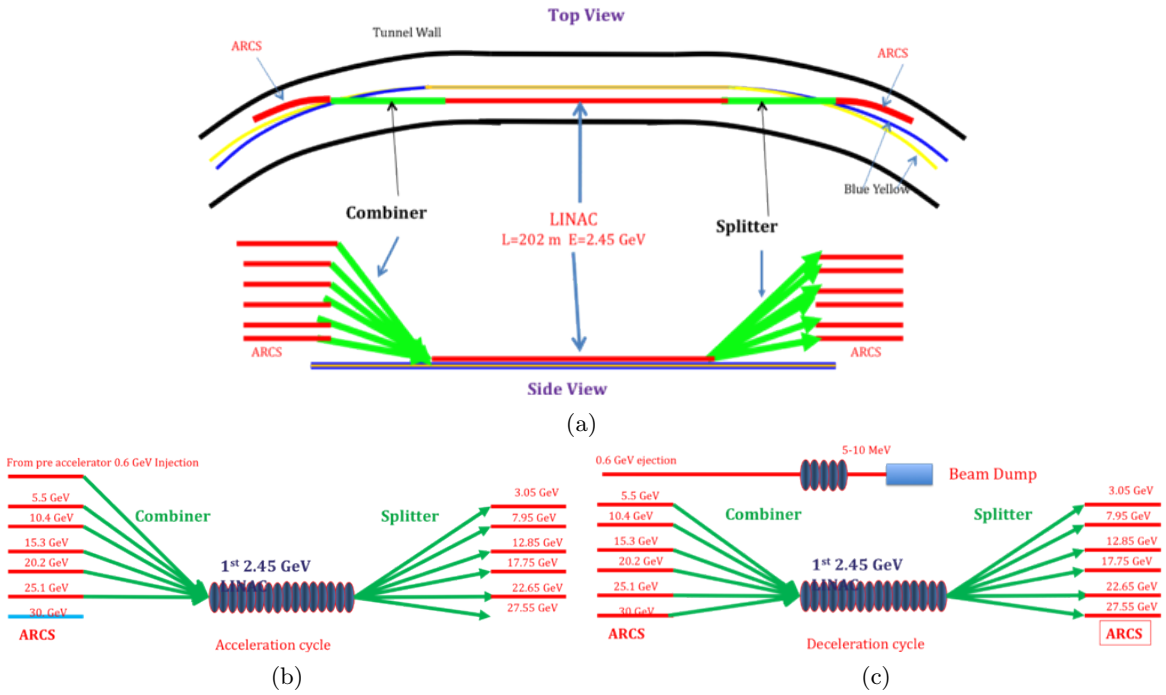

Figure 4: Scheme for the combiners and the splitters providing for 6 pass acceleration and 5 pass deceleration of the electron beam in eRHIC's ERL. The beams are separated in the vertical plane. (a) overall layout with top and side views of the 10 o'clock RHIC straight section with eRHIC linac; (b) action of the combiner and the splitter for accelerating beams; (c) action of the combiner and the splitter for decelerating beams.

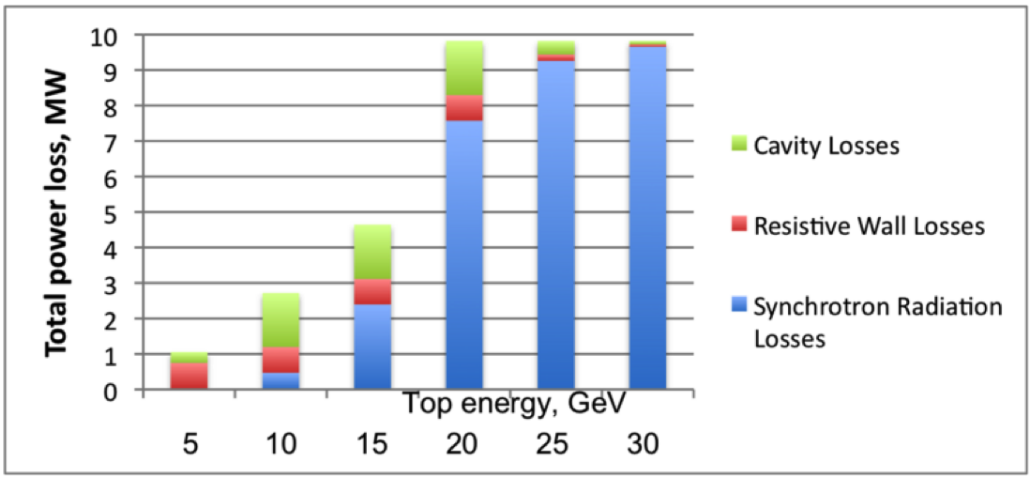

Figure 5: Electron beam power loss for various top energies of eRHIC operating with polarized electrons. Note that the losses for synchrotron radiation are kept at the fixed level for e-beam energies above 20 GeV by reducing the electron beam current proportionally to the forth power of the energy.

gains. The process of the energy recovery in SRF linacs is extremely efficient, and only about one kilowatt of RF power per 2.45 GeV linac is needed to sustain the ERL's operation.

The main beam-energy losses come from synchrotron radiation, resistive losses in the walls of vacuum chambers, and HOM losses in the SRF linacs. Figure 4 shows the values for this power loss. They must be compensated for either by a special (second-harmonic) RF system, or by special tuning of main linacs [12]. Additional non-compensated beam energy results from dumping the beam at about 5 MeV; this energy is generated by the pre-injector.

The size of the electron beam in ERL is so small that the vertical gap sizes in the arcs can be about a few

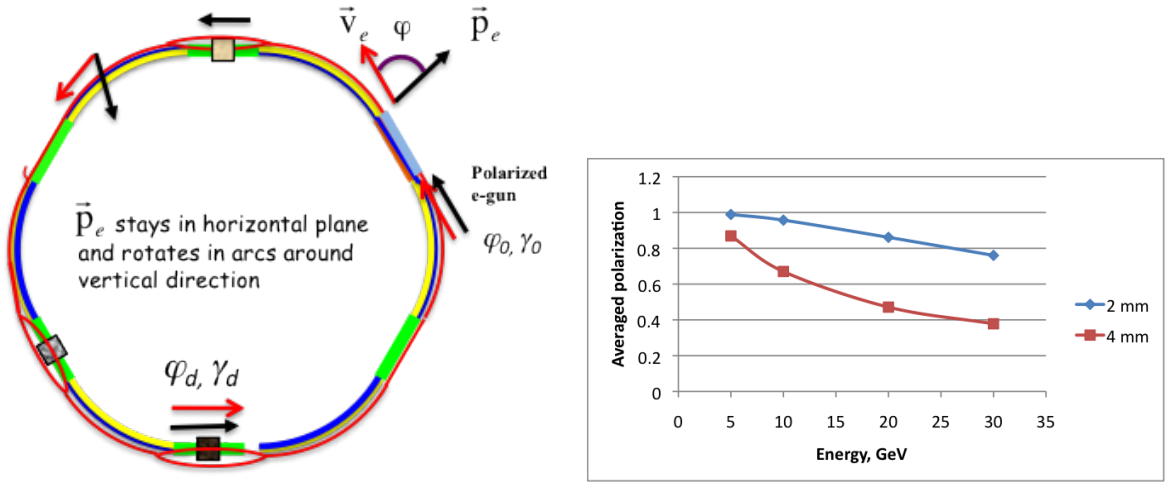

(a) (b)

Figure 6: (a) Electron spin dynamics in eRHIC; (b) degree of longitudinal polarization as function of beam energies at different bunch length.

mm; hence, using small-gap magnets is warranted. They are important cost-saving factor for eRHIC; we discuss the prototyping of such magnets in the section 5. The vacuum pipe will be made from extruded aluminum with a typical keyhole antechamber design characteristic of modern light-sources. In practice, the minimal vertical gap of the vacuum chamber (and, therefore, that of the magnets) is likely to be influenced by the tolerable wakefield effects from resistive walls and roughness. The exact value will be determined when we theoretical and experimental studies of these effects are completed.

Preserving polarization. We will preserve in the ERL the high degree of the electrons' polarization originating from the polarized electron gun [11], and provide the desirable direction, i.e., longitudinal, of the electron's polarization in the interaction point (IP). The easiest (and most economical) way of doing so is to keep the spin in the horizontal plane. In this condition, the angle between the direction of electron's velocity and its spin grows according a very simple equation:

$$\varphi(\vartheta) = \varphi_0 + \alpha \int_0^{\vartheta} \gamma(\theta)\, d\theta \tag{1}$$

where φ_0 is the initial angle at the source, ϑ is the angle of trajectory rotation in the bending magnetic field, $\gamma = E_e/m_e c^2$ is the relativistic factor of electron beam and α is anomalous magnetic moment of electron. By selecting the energy of electron providing $m\pi$ total rotation angle, where m is integer between the polarized gun and the collision point will ensure the longitudinal polarization of electrons in the IP[2]. As discussed, the direction of electron spin (helicity) will be switched by reversing the helicity of the laser photons in the gun.

With six passes in ERL and layout shown in Fig. 6, the required condition will be satisfied at IP6 for collisions at electron energies of $E_e = N \cdot 0.07216$ GeV, where N is an integer. It means that tuning energy for 0.24% of a top energy of 30 GeV will provide such a condition.

Arcs lattice. The eRHIC's arc lattice has two components, viz., that of the Blue hadron ring and the ERL lattice. The lattice of RHIC's blue ring would be modified significantly only in the IR straight sections. We discuss this in next section.

The lattice of 6-passes for eRHIC's ERL is based on a low-emittance near-isochronous lattice module. The concept of such a lattice originated from the early work of Dejan Trbojevic [13]. In addition to having an excellent filling factor, this lattice provides for fine-tuning the R56 elements in the transport matrix, so allowing perfect isochronism of the complete paths. Fig. 7 illustrates the main building block of the arc lattice. Similar blocks at the both sides of the arc lattice make it perfectly achromatic. The lattice of the regular arcs is identical for all of them, independent of their energy. The only differences arise from the splitters and combiners in the SRF linac straights, as well as from the by-pass sections in the other straights.

[2]There is no need of a transverse polarization of electrons for the physics processes of interest.

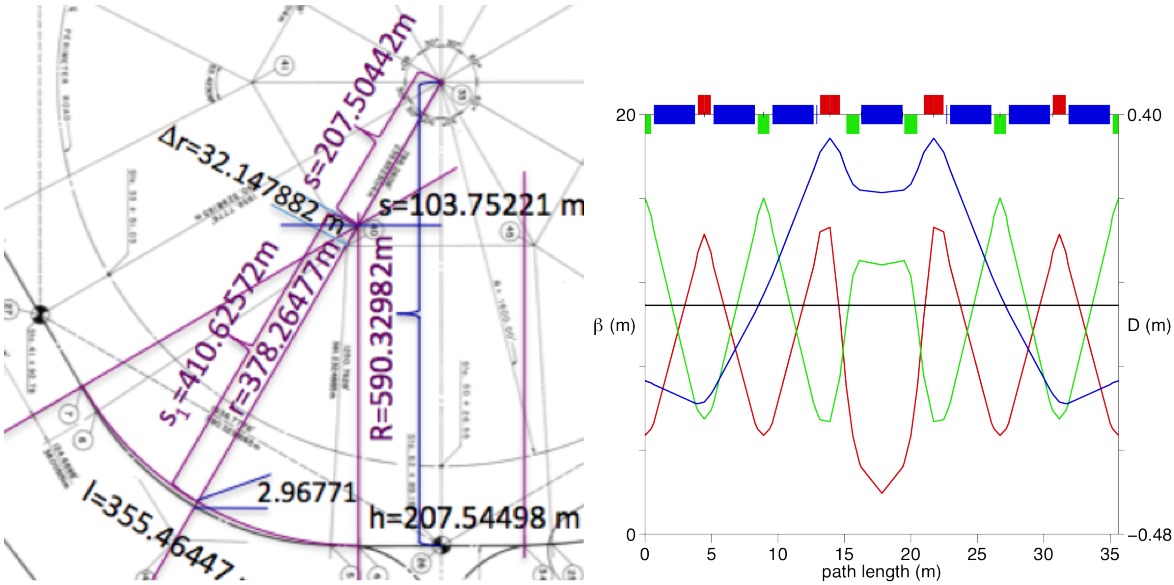

(a) (b)

Figure 7: Geometry (a), and lattice functions (b) for the standard building block.

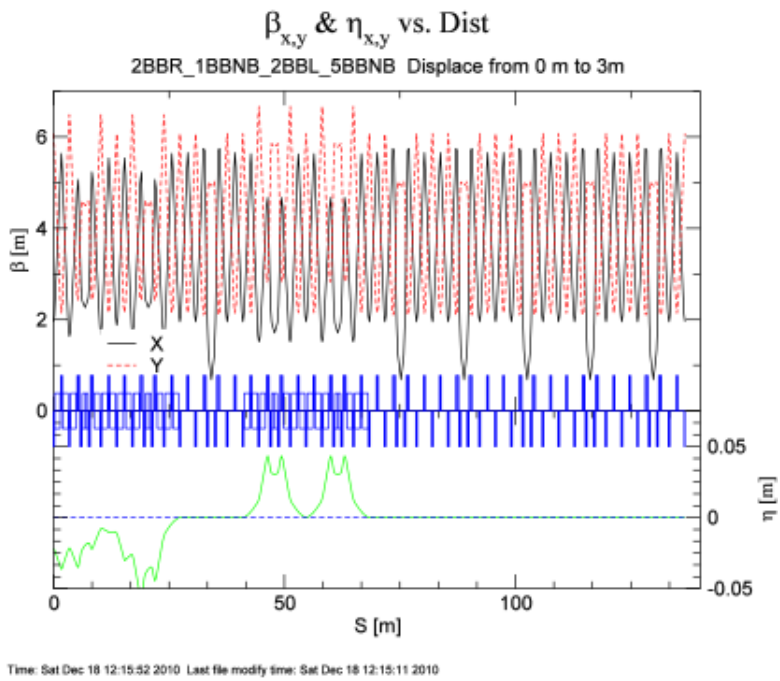

Figure 8: Half of the bilaterally symmetric lattice of the bypass around eRHIC detector at 6 o'clock.

As evident from Fig. 4, the ERL linacs will be located inside the RHIC rings, while ERL arcs are located outside them. This transition, as well as other peculiarities of the RHIC tunnel's geometry are accommodated by using two types of the same basic section (Fig.7) with slightly different radii of curvature.

Similar basic blocks are used for straight passes and for by-passes around the detectors. Fig. 8 shows such a design for the by-pass around the eSTAR detector. Presently, we are considering using a linac lattice without quadrupoles and with values of beta function of about 200 meters at its ends. Splitters and combiners serve an additional role as matching sections between linacs and arcs. Fig. 9 shows the 30 GeV splitter matching the beta functions from the linac to the arcs.

At present, the lattice of all six passes of eRHIC ERL is completed, and the exact location of each ERL

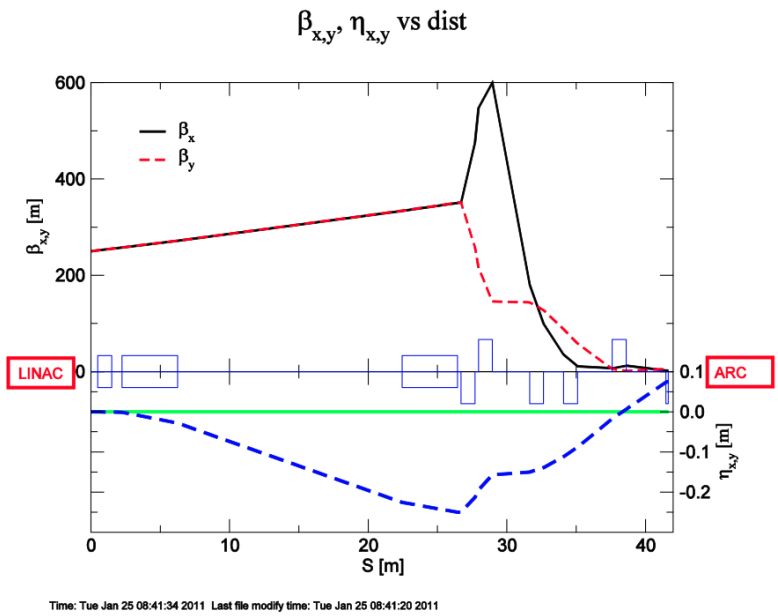

Figure 9: Lattice of the 30-GeV splitter matching the optical functions of the SRF linac and the arc.

magnet inside the RHIC tunnel identified.

One very important issue is finding a solution for synchronizing the electron beam with the hadron beam circulating in RHIC at different energies from 50- to 325-GeV/u. Being based on the ERL, eRHIC does not suffer from standard ring-ring limitations. One elegant solution identified is operating RHIC at energies corresponding to the hadron beam's repetition frequency, i.e., various sub-harmonics of the ERL RF frequency (see Fig. 10 b). The remaining tunability of the ERL's circumference can be achieved by using a standard eRHIC bypass in one of the free straight sections (for example, in IP4).

Many issues in beam dynamics for eRHIC ERL were studied and no major deterrents were found [19]. We detailed the effects of synchrotron radiation (both its energy spread and emittance growth), wakefields from SRF linacs, resistive walls, and transverse beam (TBBU) stability. We will address a few remaining questions before releasing the final eRHIC design. A remaining one is the effect of the wakefields from the wall's roughness on energy spread. These issues and possible remedies are under investigation.

4. eRHIC interaction design

Current high-luminosity eRHIC IR design incorporates a 10 mrad crab-crossing scheme; thus, hadrons traverse the detector at a 10 mrad horizontal angle, while electrons go straight through. Fig 11 plots this scheme. The hadron beam is focused to $\beta^* = 5$ cm by a special triplet wherein first magnet is a combined function magnet (1.6 m long with 2.23 T magnetic fields and a -109 T/m gradient). It has two functions; it focuses the hadron beam while bending it 4 mrad. Two other quadrupoles do not bend the hadron beam but serve only for focusing. Importantly, all three magnets provide zero magnetic fields along the electron beam's trajectory. Quadrupoles for this IR require very high gradients, and can be built only with modern superconducting technology [4,15].

This configuration guaranties the absence of harmful high-energy X-ray from the synchrotron radiation. Further, the electron beam is brought into the collision via a 130-meter long merging system (Fig. 12). The radiation from regular bending magnets would be absorbed. The last 60 meters of the merging system use only soft bends: downwards magnets have strength of 84 Gs (for 30 GeV beam) and the final part of the bend used only 24 Gs magnetic field. Only 1.9 W of soft radiation from the later magnets would propagate through the detector.

One important factor in the IR design with low $\beta^* = 5$ cm is that the chromatism of the hadron optics in the IR should be controlled, which is reflected in the maximum β function of the final focusing quadrupoles. Fig. 13a shows the designed beta and dispersion functions for hadron beam. The values of beta function are kept under 2 km, and the chromaticity held at the level typical for RHIC operations with $\beta^* \sim 1$ m. We are starting full-fledged tracking of hadron beams in RHIC, including characterizing beam-beam effects and all

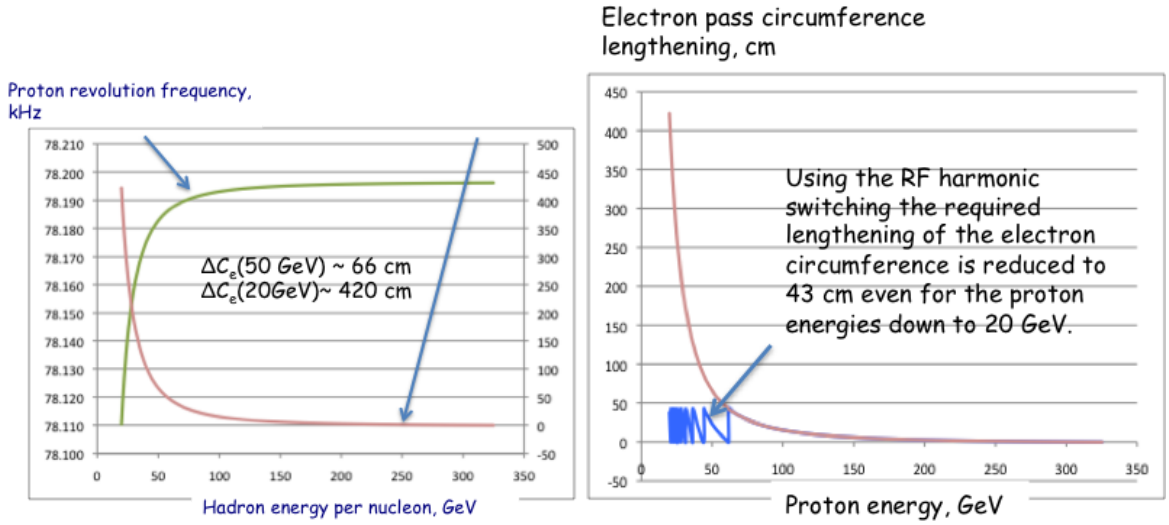

(a) (b)

Figure 10: (a) Change of the revolution frequency of hadron beams in RHIC as function of their energy; (b) Red line - the required change for the e-beam circumference without harmonic switching (i.e. ring-ring case); Blue – the same curve with switching the harmonic number.

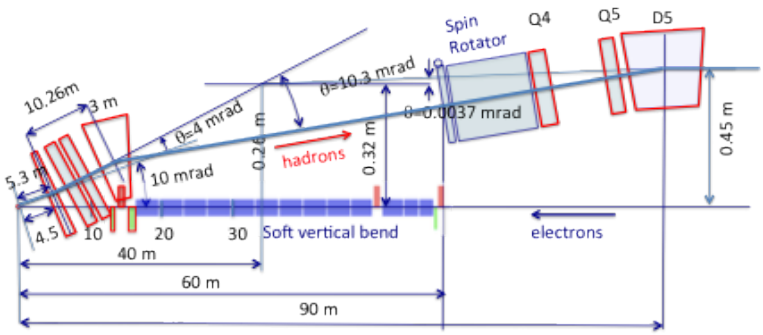

Figure 11: Layout of the right side of eRHIC IR from the IP to the RHIC arc. The spin rotator is the first element of existing RHIC lattice remaining in place in this IR design.

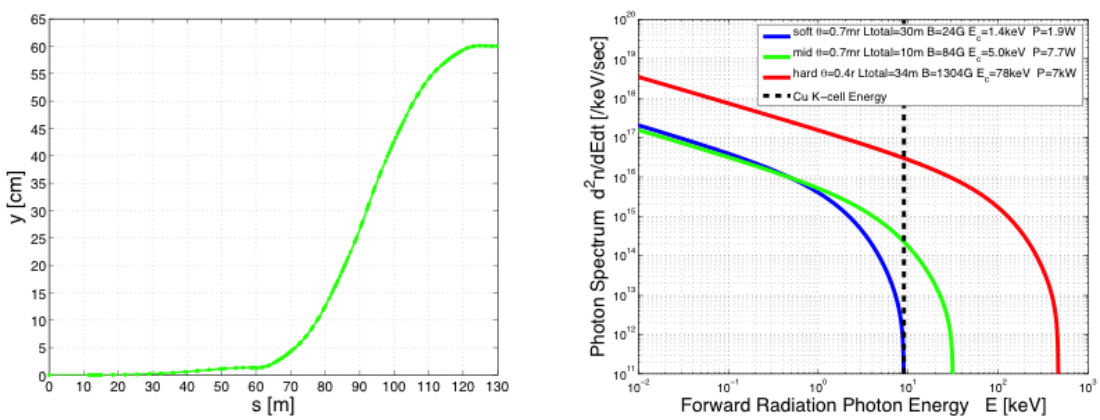

(a) (b)

Figure 12: (a) Vertical trajectory of 30 GeV electron beam merging over 130 meters into the IP. (b) Spectra of the radiation from various part of the merger. Only 1.9 W of soft X-ray radiation will propagate through the detector; the absorbers intercept the rest of it.

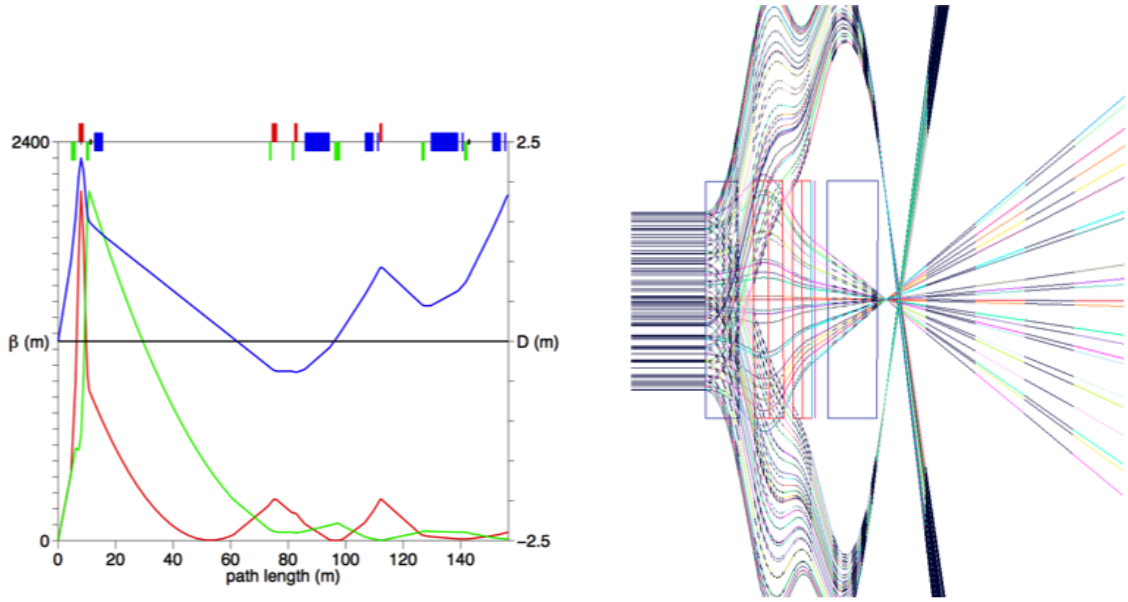

(a) (b)

Figure 13: (a) Hadron beam's optics at the eRHIC IR. The 5 cm β^* is matched into the RHIC's arc lattice that starts about 60m from the IR. (b) Tracking of hadrons with an energy deviation of +/- 0.1% through the first four magnets at the IR.

known nonlinearities of RHIC magnets: we do not anticipate any serious chromatic effects originating from our IR design.

Furthermore, we introduced the bending field in the first quadrupole for the hadrons thereby to separate the hadrons from the neutrons. Physicists considering processes of interest for EIC science requested our installing this configuration.

Since the electrons are used only once, the optics for them is much less constrained. Hence, it does not present any technical or scientific challenges, and so we omit its description here.

Finally, beam-beam effects play important role in the eRHIC's performance. While we will control these effects on the hadron beam, i.e., we will limit the total tune shift for hadrons to about 0.015, the electron beam is used only once and it will be strongly disrupted during its single collision with the hadron beam. Consequently, the electrons are strongly focused by the hadron beam (pinch effects), and the e-beam emittance grows by about a factor of two (disruption) during the collision. These effects, illustrated in Fig. 14, do not represent a serious problem, but will be carefully studied and taken into account in designing the optics and the aperture.

More details on the lattice and IR design are given in reference [16].

5. eRHIC R&D

The list of the needed accelerator R&D on the eRHIC quite extensive, ranging from the 50 mA CW polarized source to Coherent Electron Cooling [5]. It includes designing and testing multiple aspects of SRF ERL technology in BNL's R&D ERL [18].

Coherent Electron Cooling (Fig. 15) promises to cool both ion proton beams to an order on magnitude smaller beams (both transversely and longitudinally) in under a half hour. Traditional stochastic- or electron-cooling techniques could not satisfy this demand. Being a novel unverified technique, the CeC will be tested in a proof-of-principle experiment at RHIC in a collaboration between scientists from BNL, JLab, and TechX [17].

Other important R&D effort, supported by an LDRD grant, focuses on designing and prototyping small-gap magnets and vacuum chamber for cost-effective eRHIC arcs [20]. In addition to their energy efficiency and inexpensiveness, small-gap magnets assure a very high gradient as room-temperature quadrupole magnets. Fig. 16 shows two such prototypes; they were carefully tested and their fields were mapped using high-precision magnetic measurements. While the quality of their dipole field is close to satisfying our requirements, the

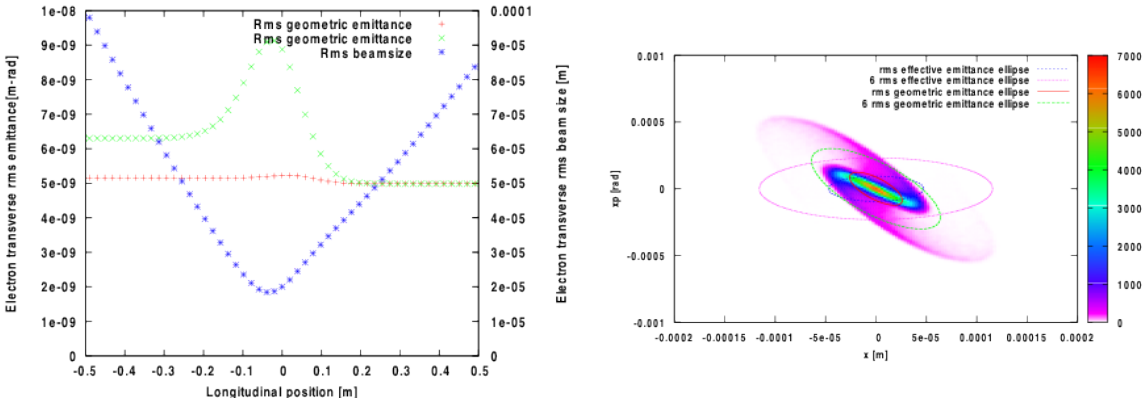

(a) (b)

Figure 14: (a) The optimized e-beam envelope during collision with the hadron beam in eRHIC; (b) distribution of electrons after colliding with the hadron beam in eRHIC.

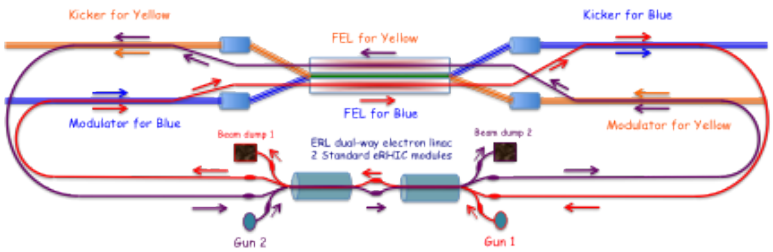

Figure 15: Possible layout of RHIC CeC system cooling for both the yellow and blue beams.

quadrupole prototype was not manufactured to our specifications. We will continue this study, making new prototypes using various manufacturers and techniques.

Another part of our R&D encompasses testing the RHIC in the various modes that will be required for the eRHIC's operation.

6. Conclusion

We are making steady progress in designing the high-energy, high-luminosity electron-ion collider eRHIC and plan to continue our R&D projects and studies of various effects and processes. So far, we have not encountered a problem in our proposed that we cannot resolve. Being ERL-based collider, eRHIC offers a natural staging

(a) (b)

Figure 16: (a) A prototype of eRHIC quadrupole with 1 cm gap; (b) Assembled prototype of eRHIC dipole magnet with 5 mm gap.

of the electron beam's energy from 5-6 to 30 GeV. During this year, we will complete our cost estimate of all eRHIC stages.

Acknowledgments

The authors would like to acknowledge contributions and advice from E.-C.Aschenauer, D.Bruhwiler, G.Bell, A.Cadwell, A.Deshpande, R.Ent, W.Gurin, A.Hutton, H.Kowalsky, , G.Krafft, M.Lamont, T.W.Ludlam, R.Milner, M.Poelker, R,Rimmer, B.Surrow, B.Schwartz, T.Ulrich, S.Vigdor, R.Venugopalan, and W.Vogelsan.

References

1 RHIC, http://www.bnl.gov/rhic/
2 eRHIC - 0th Order Design Report, Editors: M. Farkhondeh and V.Ptitsyn, BNL, 2004
3 Y.Hao et al., Proc. of First International Particle Accelerator Conference, IPAC'10, Kyoto, Japan, May 23-28, 2010, p.1614,
4 G. Ambrosio et al., Proc. of First International Particle Accelerator Conference, IPAC'10, Kyoto, Japan, May 23-28, 2010, p.403,
5 V.N.Litvinenko, Y.S.Derbenev, Physical Review Letters 102, 114801 (2009)
6 Y. Hao et al., Proc. of First International Particle Accelerator Conference, IPAC'10, Kyoto, Japan , May 23-28, 2010, pp.1617-1619,
7 E.Tsentalovich, ibid, High Intensity Polarized Electron Gun Studies at MIT-Bates
E. Tsentalovich, AIP Conference Proceedings Volume 1149,
SPIN PHYSICS: 18th International Spin Physics Symposium Charlottesville (Virginia), 6–11 October 2008, pp. 997-1001.
8 V.N.Litvinenko, Gatling Gun, Technical Note, C-AD, BNL
9 X. Chang et al., Polarized Gatling gun design, faculty.cua.edu/hornt/EICC_CUA_2010/.../Chang_Gatling_gun_design.ppt
10 R. Calaga et al., Physica C 441 (2006) 159-172
11 V.N. Litvinenko et al., Proc. of 2005 Particle Accelerator Conference, May 2005, Knoxville, TN, 2768
12 Using main linacs to compensate for synchrotron radiation losses in high energy ERLs, Vladimir N. Litvinenko, in submission process
13 D.Trbojevic et al, AIP CONFERENCE PROCEEDINGS, V. 530, (2000) p. 333
14 Y. Hao et al., Proceedings of 2009 Particle Accelerator Conference, Vancouver, Canada, May 4-8, 2009,
15 P. Wanderer, IEEE Appl. Superconductivity, Vol. 19, no. 3, June 2009, pp. 1208-1211.
16 D. Trbojevic et al., Proceedings of IPAC'10, Kyoto, Japan, May 2010.
17 DoE NP offices support this R&D project starting in FY 2011.
18 D. Kayran et al., Proc XXIV Linear Accelerator Conf. (LINAC08), Victoria, BC, Canada, September 29-October 3, 2008.
19 G. Wang et al., Proceedings of First International Particle Accelerator Conference, IPAC'10, Kyoto, Japan, May 23-28, 2010.
20 Yue Hao et al., Proceedings of First International Particle Accelerator Conference, IPAC'10, Kyoto, Japan, May 23-28, 2010.